Analysis and automatic inversion of the HVSR curve with HoliSurface® 2025: a short example

INDEX

1.1 Geological Setting

The study area is located in the eastern sector of the *Bassa Pianura Friulana* (northeastern Italy). From a lithological perspective, the local sediments belong to the Würm glaciation and the recent post-glacial period.

Following a transitional phase and the glacier's retreat from the moraine amphitheater, meltwaters converged along the present course of the Tagliamento River, forming the Friulian sedimentary plain, likely with significant contributions from the Isonzo and Natisone fluvio-glacial systems. Post-glacial floods from the Torre and Natisone rivers repeatedly reworked the sediments, depositing new alluvial layers.

In the eastern sector this region, the bedrock outcrops east of Monfalcone, while depths increase toward the western plain, probably reaching up to around 900 m (Figure 1).

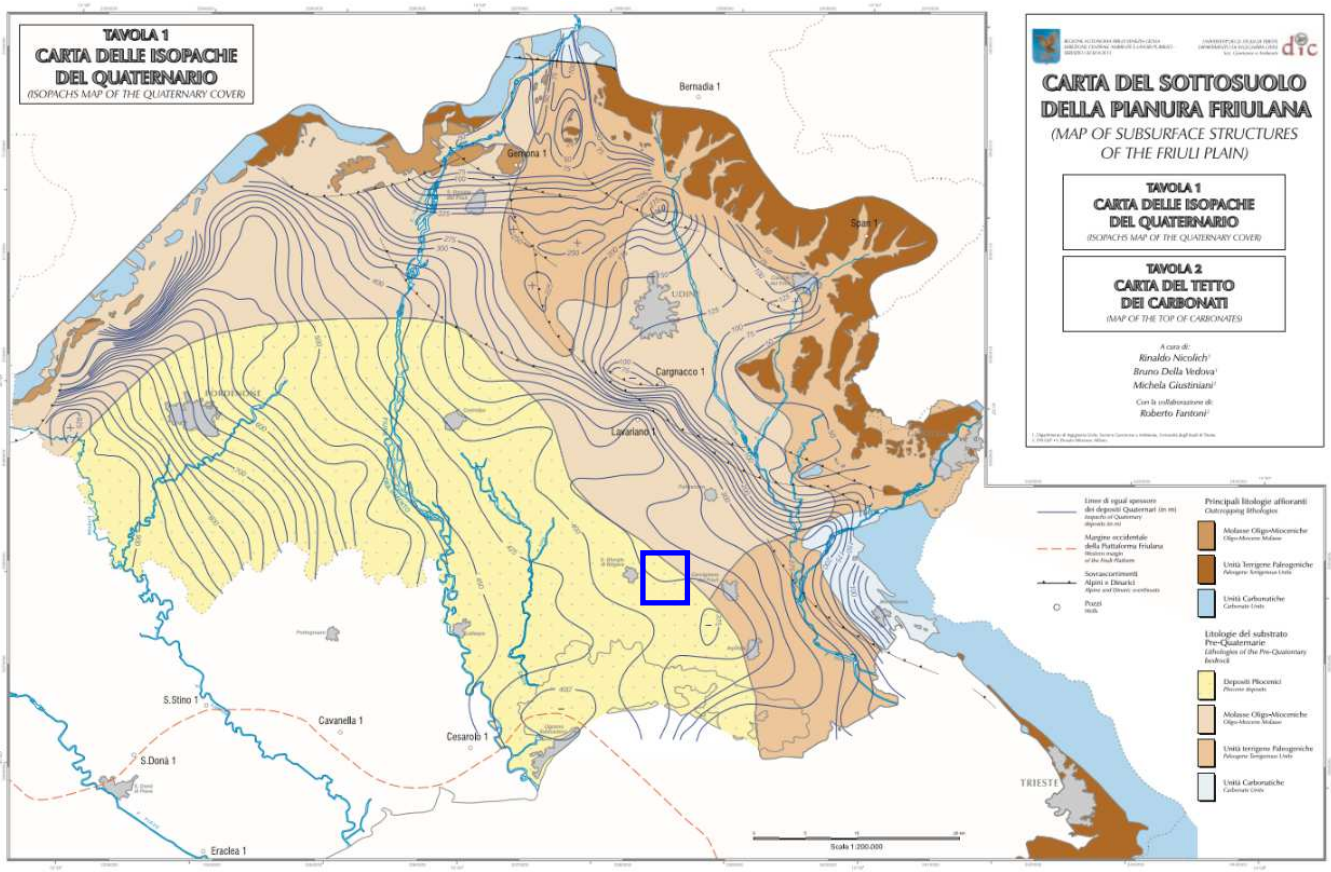

Figure 1. Isopach map of Quaternary deposits (Friuli Venezia Giulia – Geological Service).

1.2 HVSR (*Horizontal-to-Vertical Spectral Ratio*): a brief introduction

The HVSR (*Horizontal-to-Vertical Spectral Ratio*) curve has been used in seismology roughly since the late 1960s (see, for example, Mark & Sutton, 1975). A clear and universally valid relationship between the HVSR and the so-called site amplification has never been clearly established, either theoretically or experimentally. In fact, theoretical considerations and experimental observations do not support the widely held idea that the HVSR represents, by itself, the site amplification.

Several studies have shown that (see, for example, Perron et al., 2018, and the references therein) the actual amplification recorded during an earthquake can differ significantly from the HVSR curve (see, for example, the data shown in Figure 2).

Therefore, although when used together with surface-wave velocity data, HVSR represents a valuable tool for estimating the shear-wave velocity (V_S) of the deeper layers (e.g., Arai & Tokimatsu, 2005; Dal Moro, 2020), it should not be simplistically interpreted as a direct estimate of site amplification.

The “deformation” phenomena of the ground motion generated by a seismic event are complex and do not depend solely on the site conditions but also on the characteristics of the seismic event itself. The same site may respond differently depending on the properties of the considered event (see bibliographic references reported in Dal Moro, 2020).

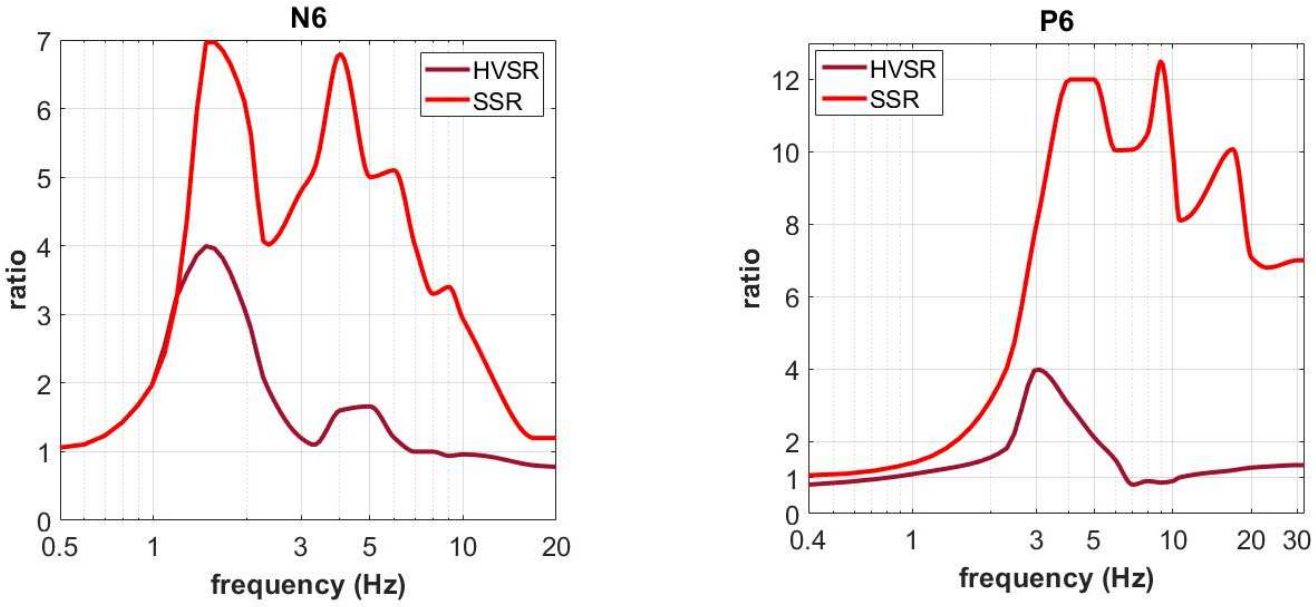

Figure 2. Comparison between the HVSR curve and the actual mean amplification computed during a series of seismic events by means of the SSR (*Standard Spectral Ratio analysis*) technique (from Perron et al., 2018). Note the significant discrepancy between the HVSR and the amplification actually measured.

1.3 HVSR computation

The images in this section summarize the key characteristics of the microtremor field used to compute the HVSR at the investigated site (total recording time: ~24 minutes). The presence of a couple of narrow-band **industrial components** (visible in the unsmoothed amplitude spectra in Figure 4) does not significantly affect the HVSR curve (Dal Moro, 2020; 2025). If necessary, their influence could have been easily mitigated using the *detection and removal tool* available in **HoliSurface®**.
The HVSR peak at 2.25 Hz reflects the impedance contrast between the loosely compacted near-surface sediments and the more densely compacted deposits that are well documented in the study area.

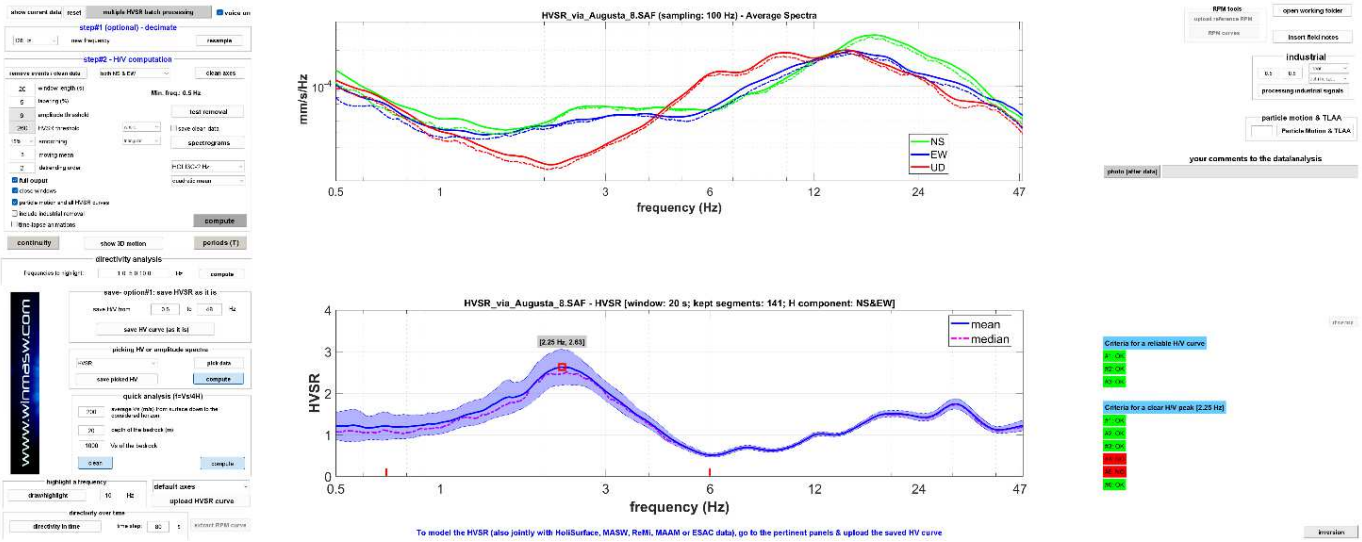

Figure 3. HVSR – Amplitude spectra of the three components and mean HVSR curve.

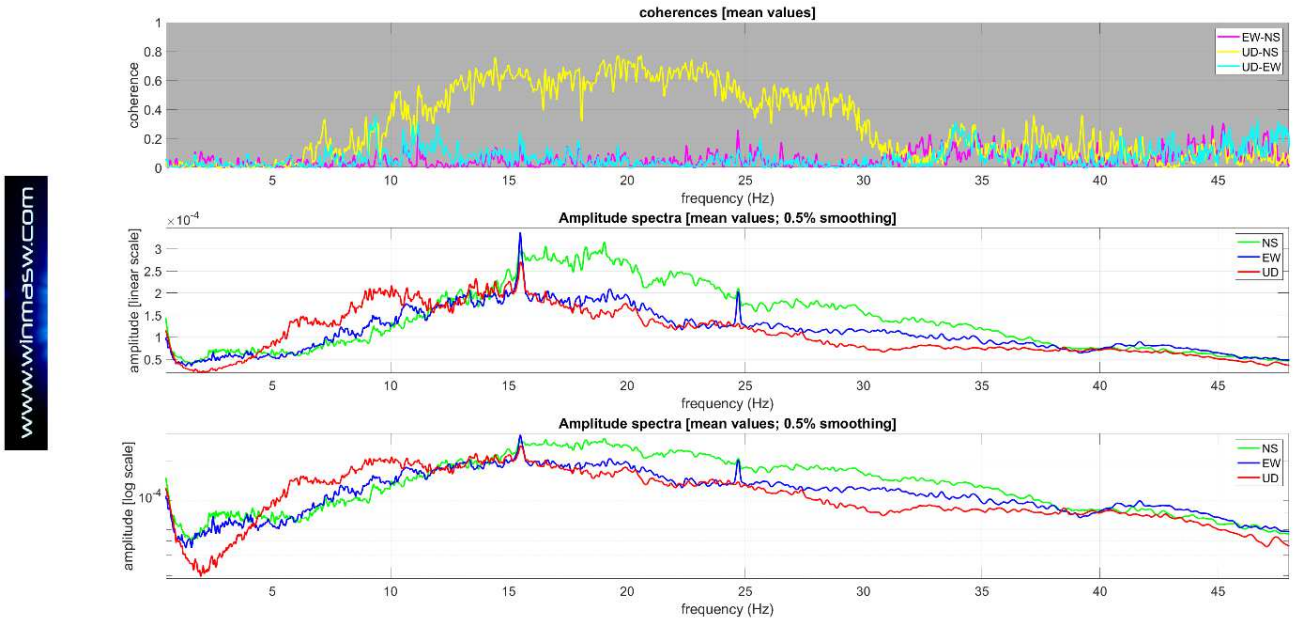

Figure 4. Coherence functions for the three sensor combinations and amplitude spectra smoothed by only 0.5%. Two minor monochromatic industrial components (at approximately 15.5 and 24.5 Hz) can be observed, which, as clearly shown by the data shown in Figure 3, do not significantly affect the HVSR.

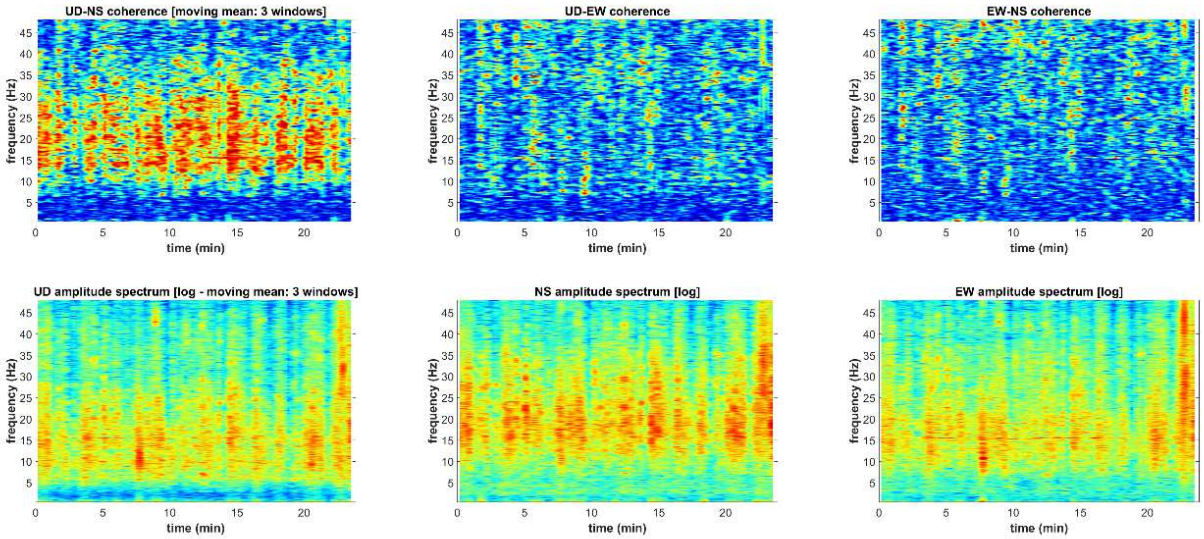

Figure 5. HVSR: coherence functions for all the sensor combinations (UD-NS, UD-EW, EW-NS – upper graphs) and amplitude spectra (lower graphs) over time: no phenomena of particular relevance are observed during the data acquisition.

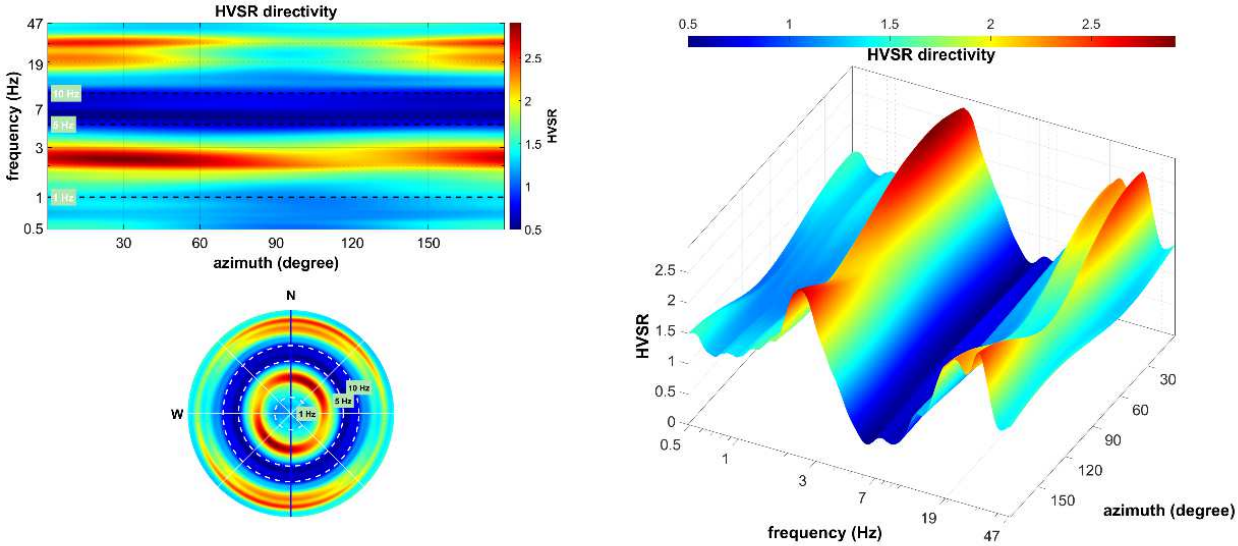

Figure 6. HVSR directivity: the analysis indicates only a slight directivity (se also Figure 7).

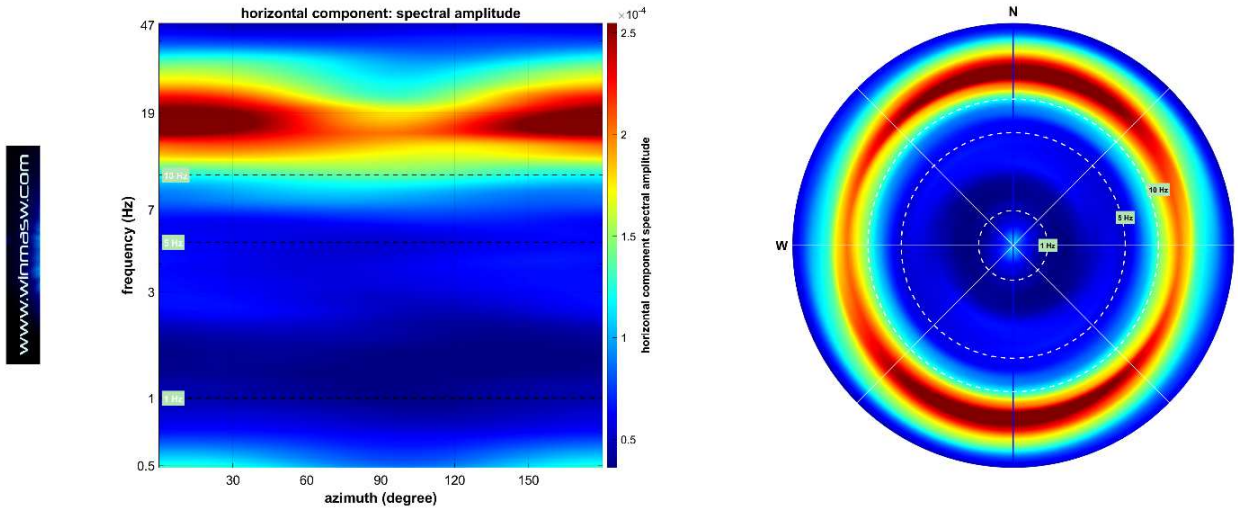

Figure 7. Azimuthal distribution of microtremor amplitude on the horizontal plane. The minor directivity of the horizontal component is responsible for the minor HVSR directivity shown in Figure 6.

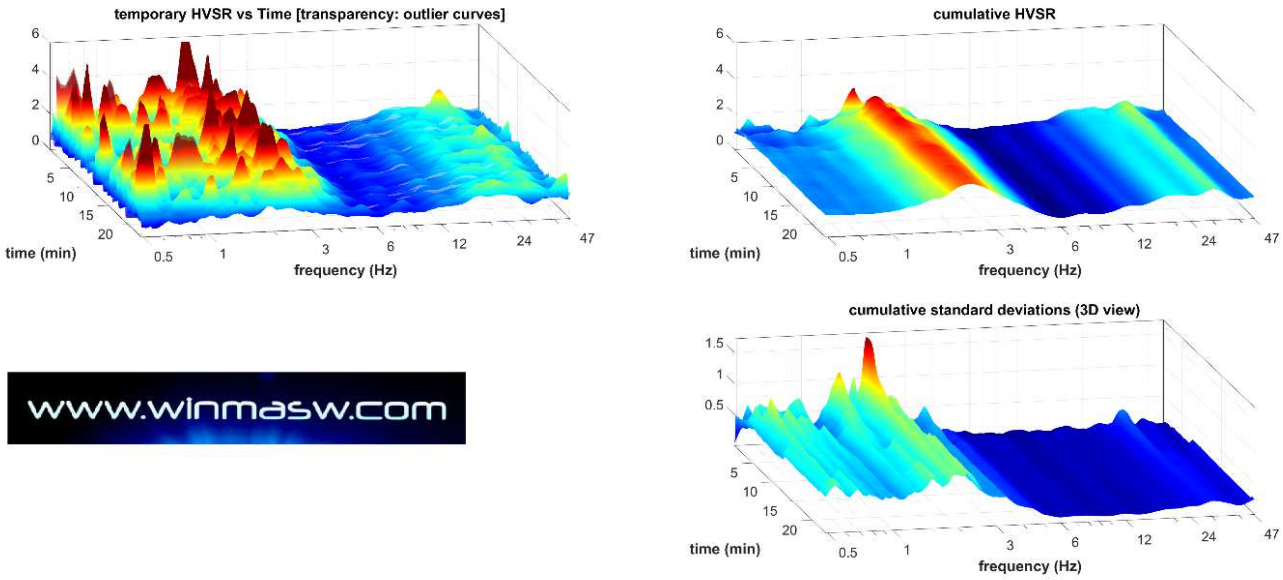

Figure 8. HVSR and standard deviation over time (time lapse analysis).

1.4 Constrained inversion of the HVSR curve

The obtained HVSR curve was ultimately inverted based on the information from a penetrometer test and the knowledge of the local general stratigraphic conditions, with constraints on layer thicknesses and on maximum and minimum V_S values fixed for each layer accordingly). We must also consider that, over the years, this area has been extensively characterized also considering dispersion data (i.e., surface-wave velocities).

The inversion was performed using a heuristic optimization procedure based on **Genetic Algorithms (GA)** as implemented in **HoliSurface®** 2025. The obtained model is shown below (Figure 9).

An excellent fit is observed between the measured HVSR and the synthetic curve associated to the identified model. This agreement is meaningful only in light of the applied constraints, since it is well known that HVSR inversion alone is subject to strong non-uniqueness.

As for the relatively stiff near-surface layer, a possible correlation with the well-documented Roman subsurface archaeological structures at this site can be reasonably hypothesized.

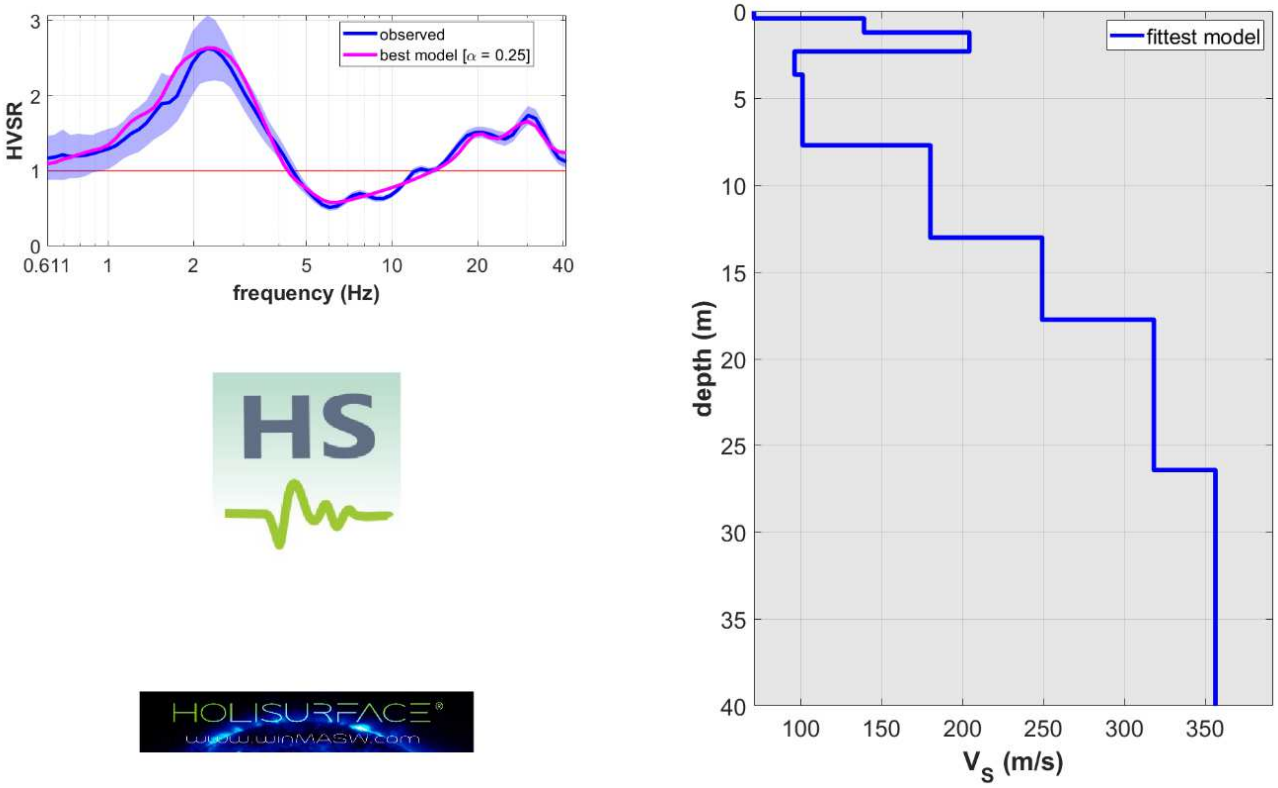

Figure 9. Result of the constrained inversion of the HVSR curve

Vs (m/s): 71, 139, 204, 96, 101, 180, 249, 318, 356, 409, 369, 922

Thickness (m): 0.4, 0.8, 1.1, 1.3, 4.1, 5.3, 4.7, 8.7, 21.9, 23.3, 341.7

Estimated densities (gr/cm^3): 1.56 1.74 1.84 1.64 1.65 1.81 1.9 1.96 1.99 2.03 2 2.25

Vs_{30} & Vs_{eq} (m/s): 191 191

1.5 References

Arai, H., Tokimatsu, K., 2005. *S-Wave velocity profiling by joint inversion of microtremor dispersion curve and horizontal-to-vertical (H/V) spectrum*. Bull. Seism. Soc. Am. 95, 1766–1778

Dal Moro, G., 2020. ***Efficient Joint Analysis of Surface Waves and Introduction to Vibration Analysis: Beyond the Clichés***, Springer, ISBN 978-3-030-46303-8

Dal Moro G., 2020. ***On the identification of industrial components in the Horizontal-to-Vertical Spectral Ratio (HVSR) from microtremors.*** Pure and Applied Geophysics, https://doi.org/10.1007/s00024-020-02424-0

Dal Moro G., 2025. ***Possible Effects of Industrial Components on the Miniature Array Analysis of Microtremors and Horizontal-to-Vertical Spectral Ratio (with Some Notes on Their Joint Inversion).*** Pure and Applied Geophysics, https://doi.org/10.1007/s00024-025-03736-9

Mark, N., Sutton, G.H., 1975. *Lunar shear velocity structure at Apollo sites 12, 14, and 15*. J. Geophys. Res. 80, 4932–4938

Perron V., Gélis C., Froment B., Hollender F., Bard P.-Y., Cultrera G., Cushing E.C., 2018. *Can broad-band earthquake site responses be predicted by the ambient noise spectral ratio? Insight from observations at two sedimentary basins*. Geophysical Journal International, 215, 1442–1454